RICH 2025

12th International Workshop on Ring Imaging Cherenkov Detectors – Mainz (Germany), 15 – 19 September 2025

Performance of the High Momentum Particle IDentification (HMPID) detector during LHC Run 3

Giacomo Volpe* for the ALICE collaboration

**University and INFN, Bari, Italy*

ALICE

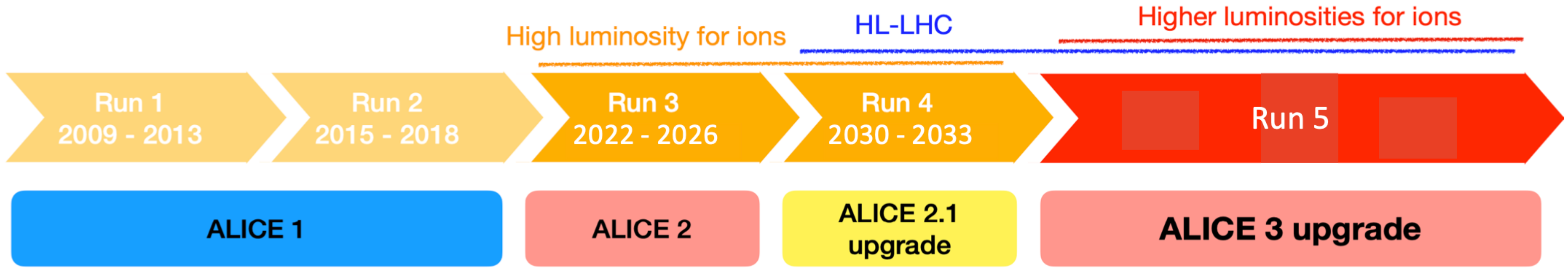

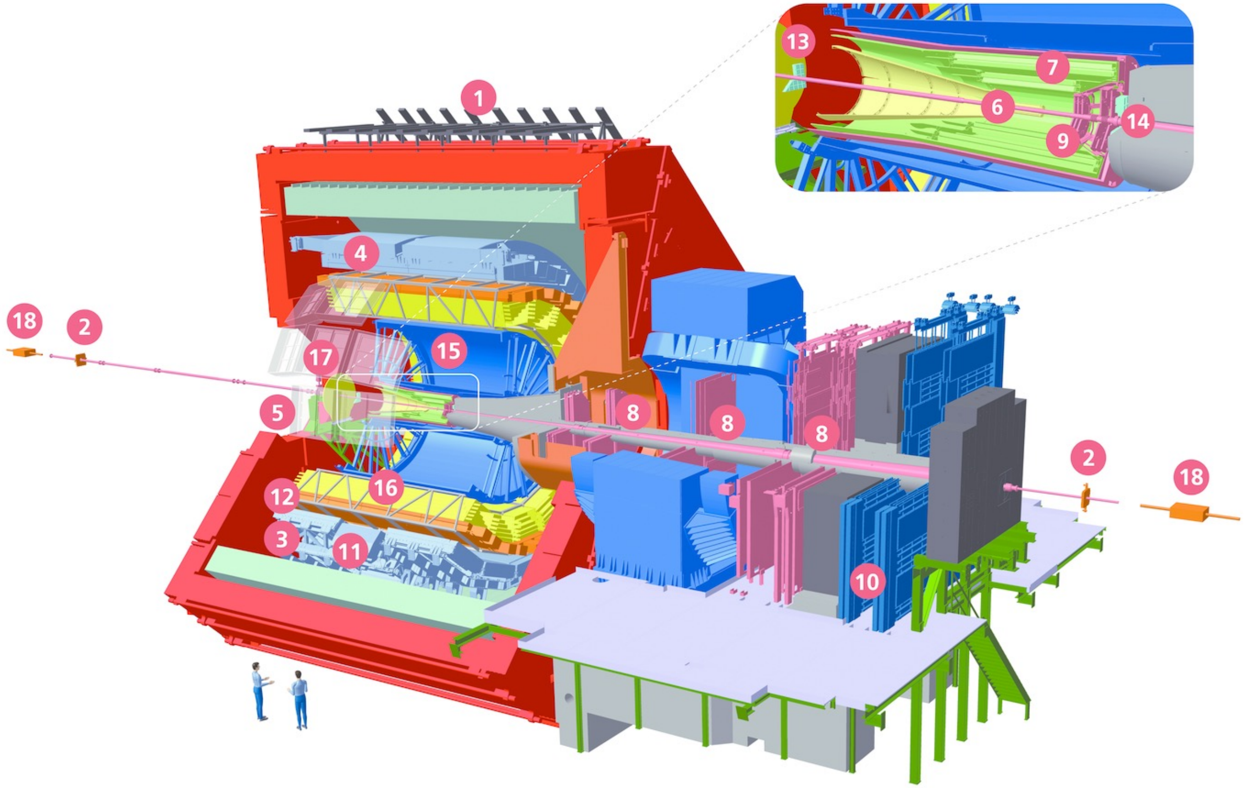

1. **ACORDE** | ALICE Cosmic Rays Detector
2. **AD** | ALICE Diffractive Detector
3. **DCal** | Di-jet Calorimeter
4. **EMCal** | Electromagnetic Calorimeter
5. **HMPID** | High Momentum Particle Identification Detector
6. **ITS-IB** | Inner Tracking System - Inner Barrel
7. **ITS-OB** | Inner Tracking System - Outer Barrel
8. **MCH** | Muon Tracking Chambers
9. **MFT** | Muon Forward Tracker
10. **MID** | Muon Identifier
11. **PHOS / CPV** | Photon Spectrometer
12. **TOF** | Time Of Flight
13. **T0+A** | Tzero + A
14. **T0+C** | Tzero + C
15. **TPC** | Time Projection Chamber
16. **TRD** | Transition Radiation Detector
17. **V0+** | Vzero + Detector
18. **ZDC** | Zero Degree Calorimeter

ALICE is designed to study the physics of strongly interacting matter under extremely high temperature and energy densities to investigate the properties of the **quark-gluon plasma**.

ALICE

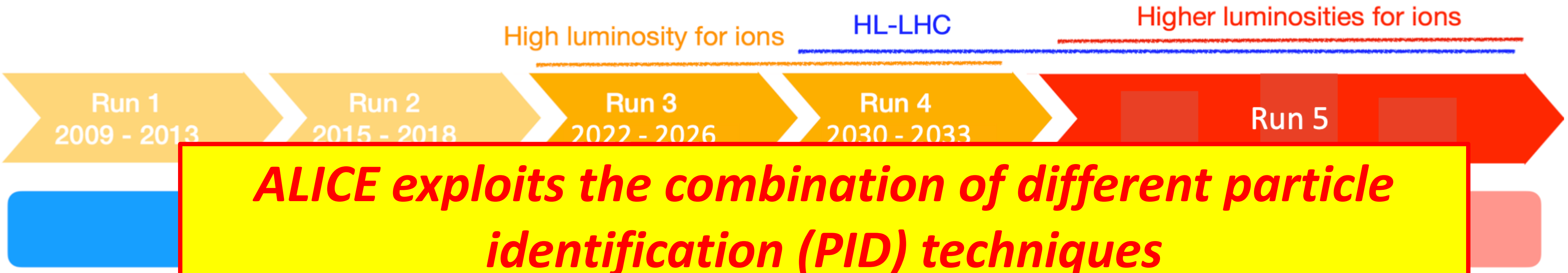

ALICE exploits the combination of different particle identification (PID) techniques

- Energy loss (ITS, TPC)
- Time of flight (TOF)
- **Cherenkov radiation (HMPID)**
- Transition radiation (TRD)
- Calorimeters (EMCal/DCal, PHOS)
- Topological PID

d to study the
gly interacting
xtremely high
and energy
vestigate the
e **quark-gluon**

13 **T0+A** | Tzero + A
14 **T0+C** | Tzero + C
15 **TPC** | Time Projection Chamber
16 **TRD** | Transition Radiation Detector
17 **V0+** | Vzero + Detector
18 **ZDC** | Zero Degree Calorimeter

HMPID detector description

The ALICE-HMPID (**H**igh **M**omentum **P**article **I**dentification **D**etector) performs charged particle track-by-track identification by means of the measurement of the emission angle of Cherenkov radiation and of the momentum information provided by the tracking devices.

It consists of seven identical proximity focusing RICH counters.

RADIATOR
15 mm liquid C_6F_{14},
n ~ 1.2989 @ 175nm, β_{th} = 0.77

PHOTON CONVERTER
Reflective layer of CsI
QE ~ 25% @ 175 nm.
The largest scale (11 m^2) application of CsI photo-cathodes in HEP
≈ 5 % of TPC acceptance

PHOTOEL. DETECTOR
- MWPC with CH_4 at atmospheric pressure (4 mm gap) HV = 2050 V.

- Analogue pad readout

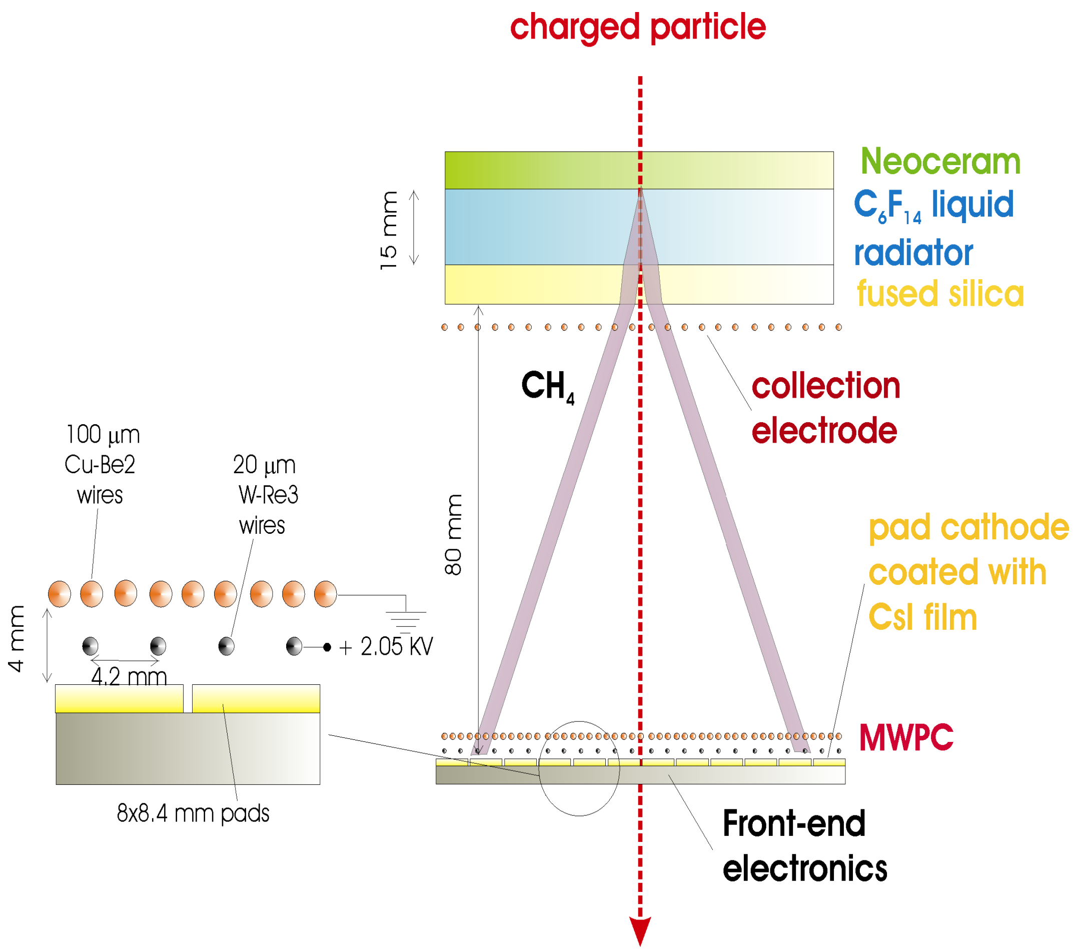

Some physics results from Run 1 and 2 with HMPID contribution

π, K, p and light nuclei spectra, resulting from the combination of the information provided by 5 different analyses (dE/dx, TOF, Cherenkov, kinks topology for kaons).

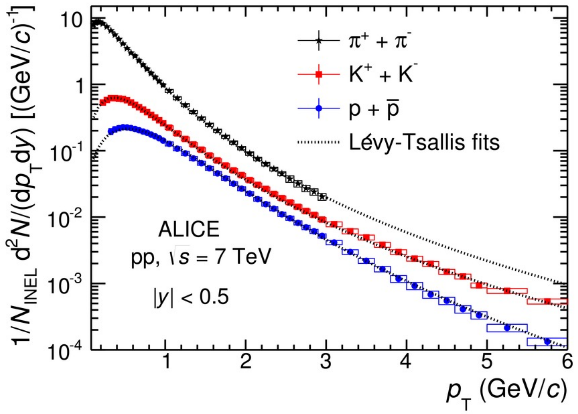

[ALICE Coll., Eur. Phys. J. C (2015) 75:226](#)

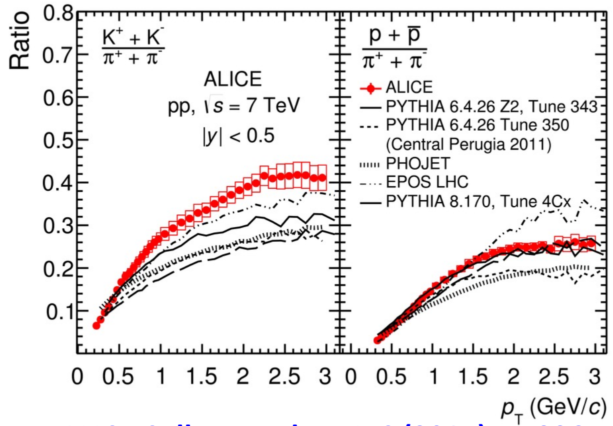

[ALICE Coll., Eur. Phys. J. C (2015) 75:226](#)

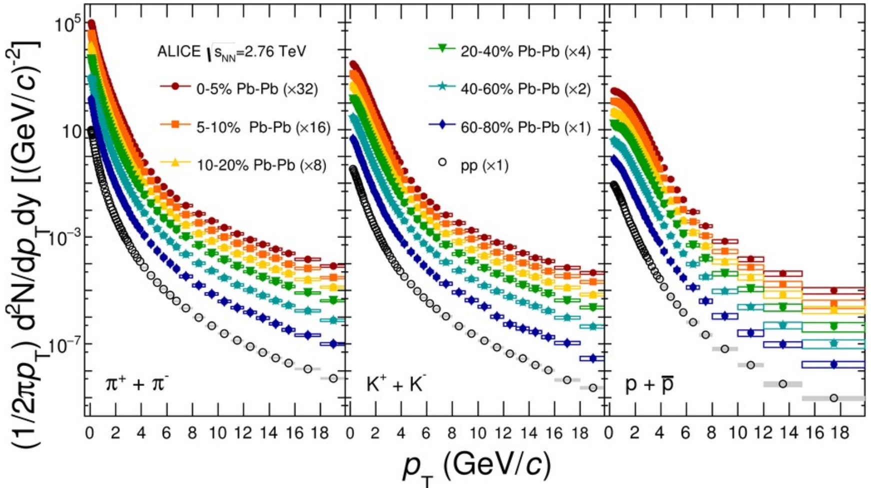

[ALICE Coll., PHYSICAL REVIEW C 93, 034913 (2016)](#)

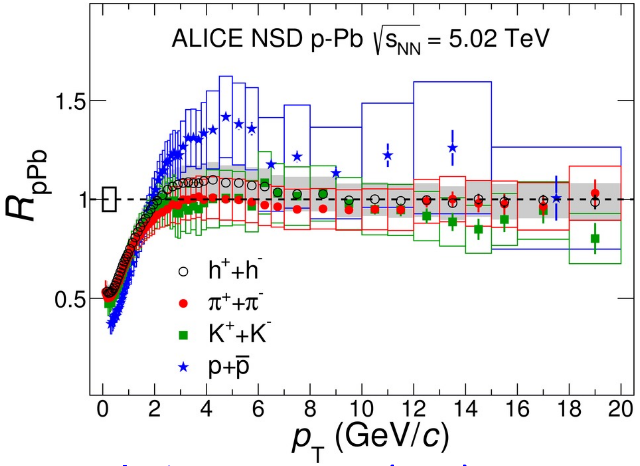

[Physics Letters B 760 (2016) 720–735](#)

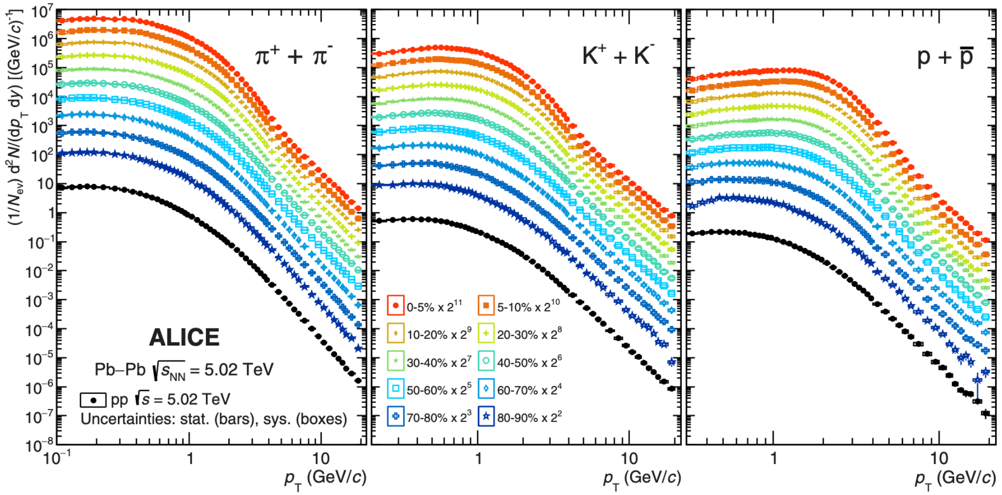

[ALICE Coll., PHYSICAL REVIEW C 101, 044907 (2020)](#)

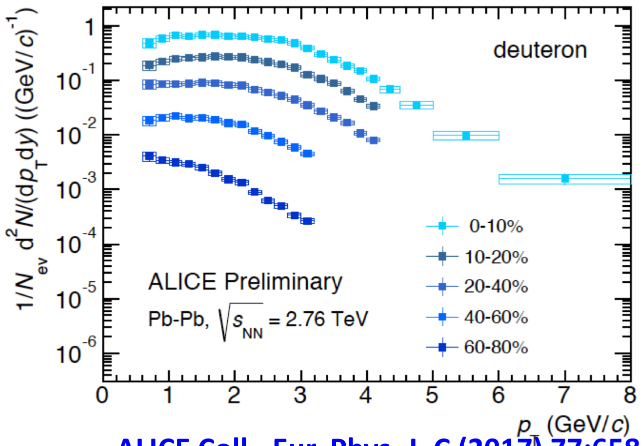

[ALICE Coll., Eur. Phys. J. C (2017) 77:658](#)

HMPID detector status 2025

Leaking radiator vessel

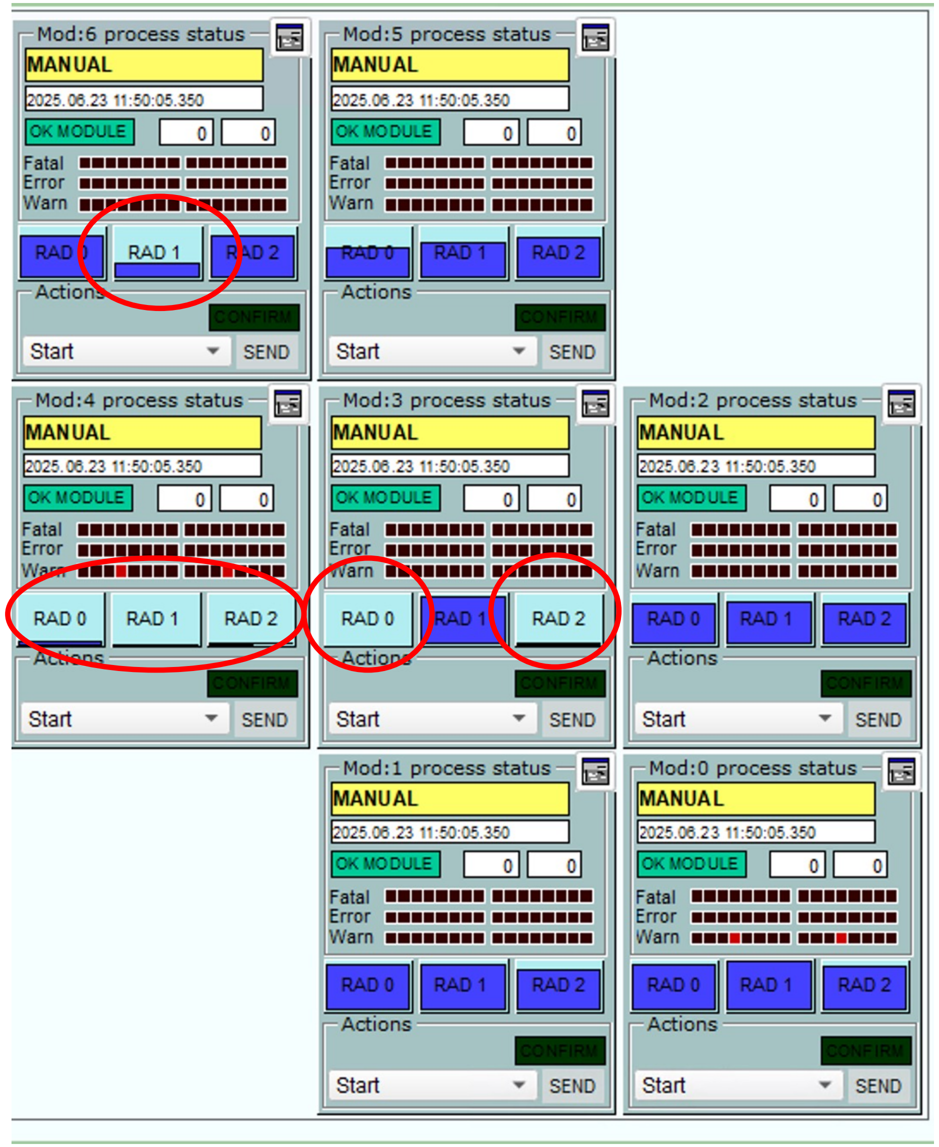

Failing HV sectors

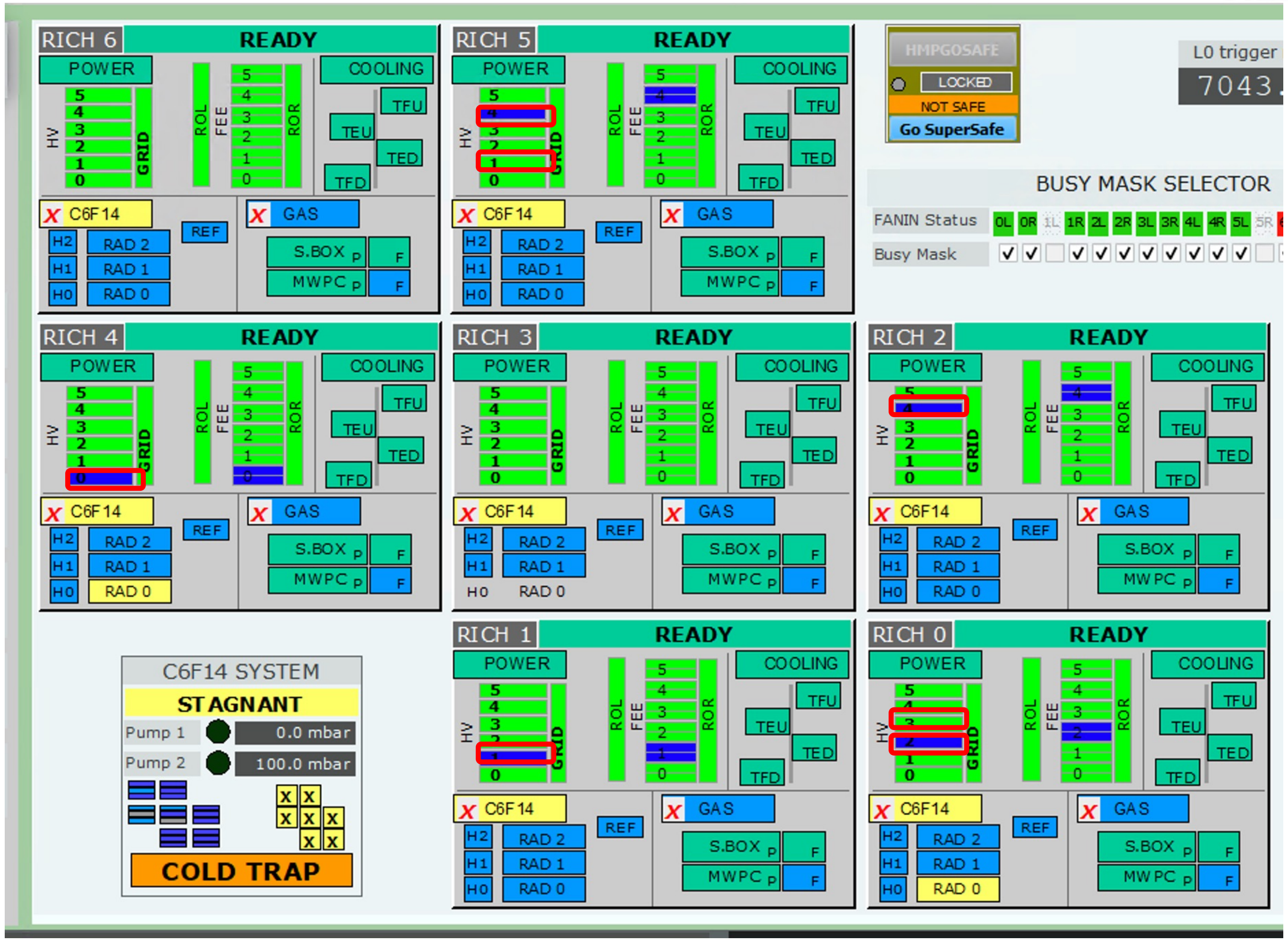

Faulty sub-system segments: Combining leaking vessels and failing HV sectors, the detector acceptance is ≅ 60%

Detector upgrading for Run 3

- New RO firmware increased the read-out data rate

Readout rate vs. occupancy

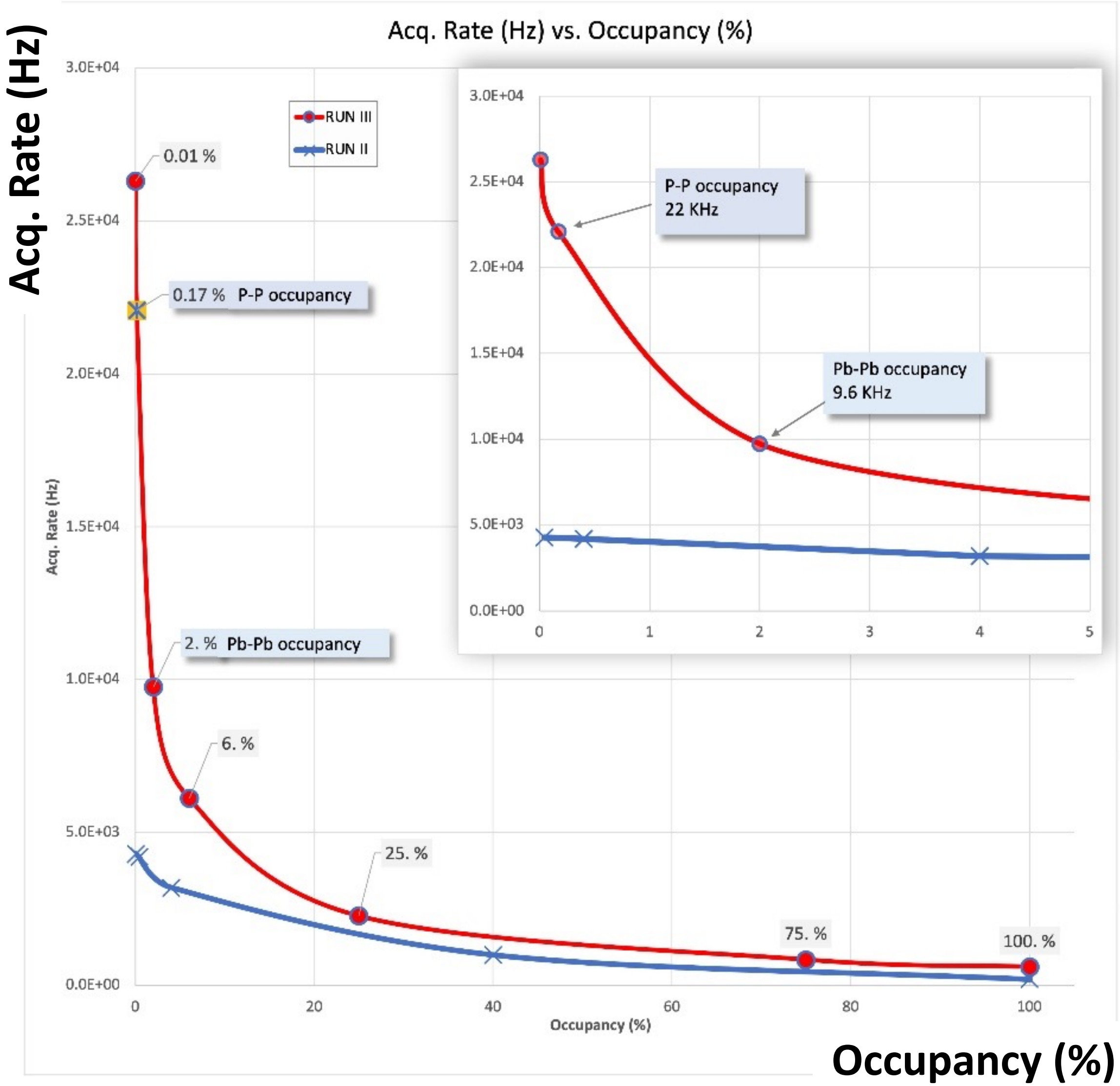

Detector stability: MWPCs gain

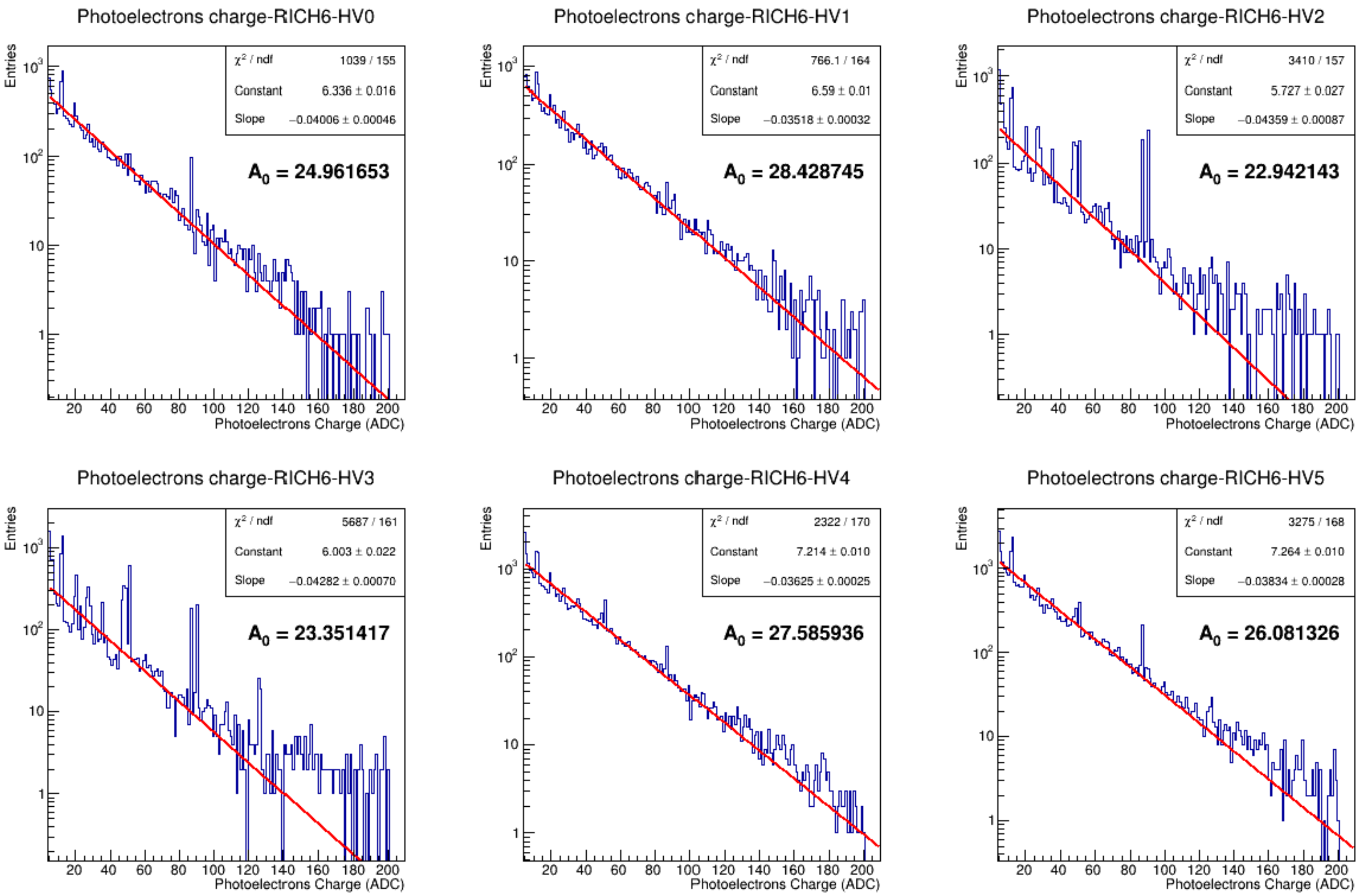

Photo-electron pulse height distribution

$$\boxed{P(A) = \frac{1}{A_0} e^{-A/A_0}}$$

The A_0 parameter is an estimator of the MWPC gain.

Detector stability: MWPCs gain

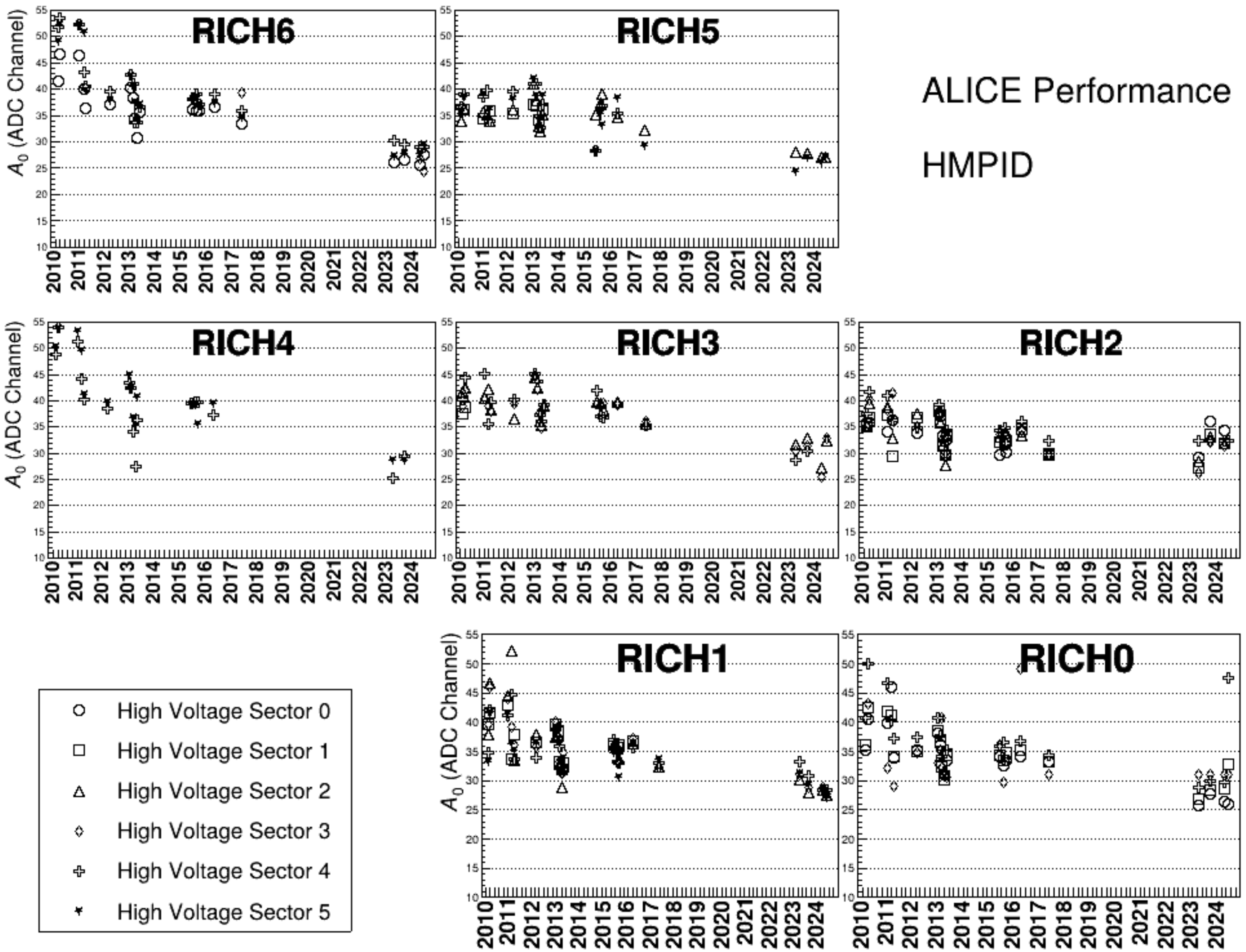

HV equalization (Sept. 2011) to set $A_0 \approx 35$;

In general gain variations ≈ ± 15%;

On average in Run 3 the gain is lower than that in Run 1-2

- missing radiator vessels
- Chamber aging after more than 15 year of operation → gas polymerization on anode wires

A reduction of 20% on A_0 → photoelectron detection efficiency loss of 3% ($A_{th}/A_0 \approx 4/35$) .
No effects on the PID performance!

Detector stability: number of detected ph.e. at saturation

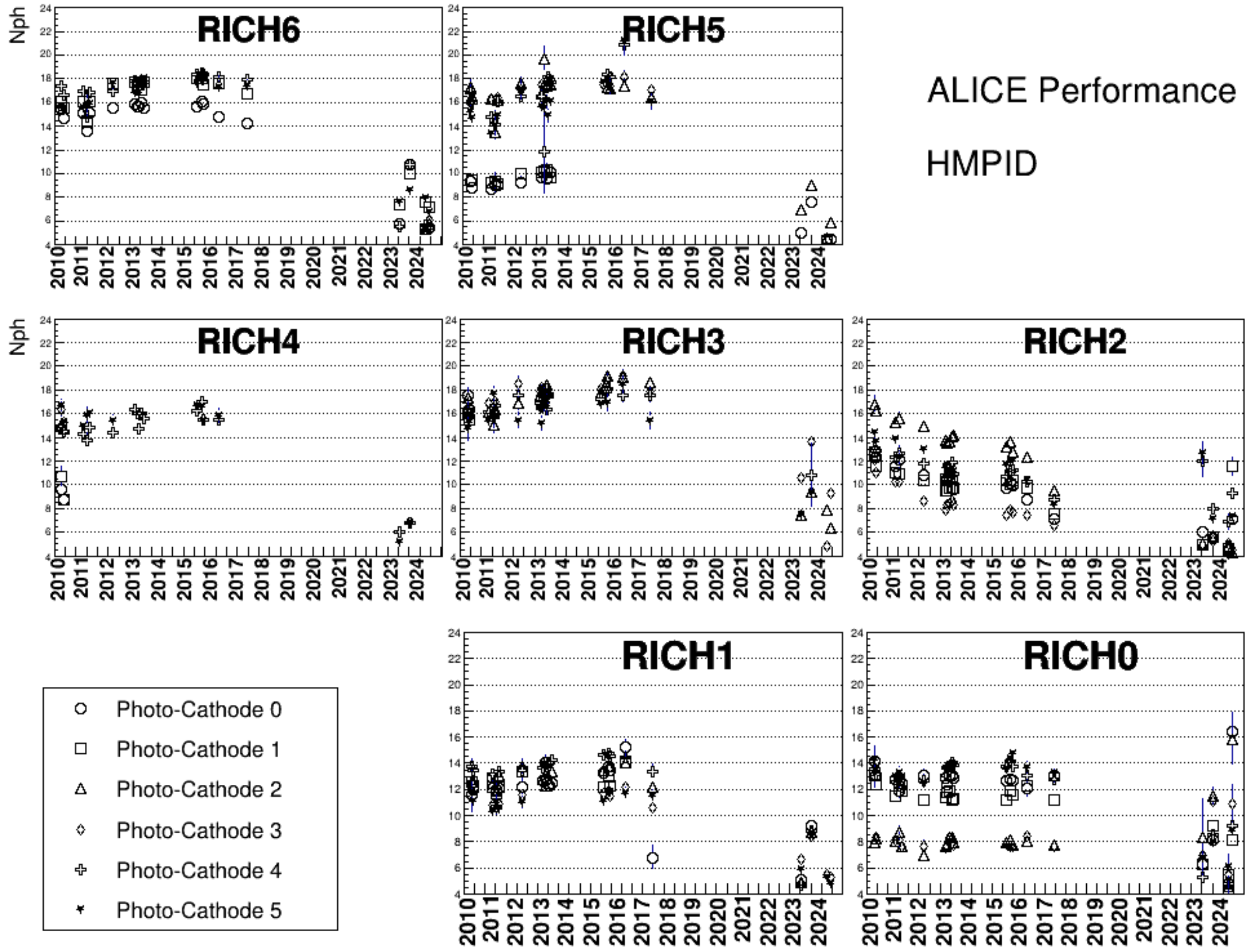

Good N_{ph} stability In Run 1-2 infers a CsI QE stability;

- Except RICH2, where PC2 and PC3 show a drop of 30%. After cleaning, these PCs were re-evaporated during 2005, maybe procedure not optimised;

On average in Run 3 the N_{ph} is lower than that in Run 1-2

- missing radiator vessels and failing HV sector decrease the full circle Cherenkov rings
- CsI aging effect after more than 15 year of operation → radiation damage.

CsI radiation damage: specific charge dose vs. time

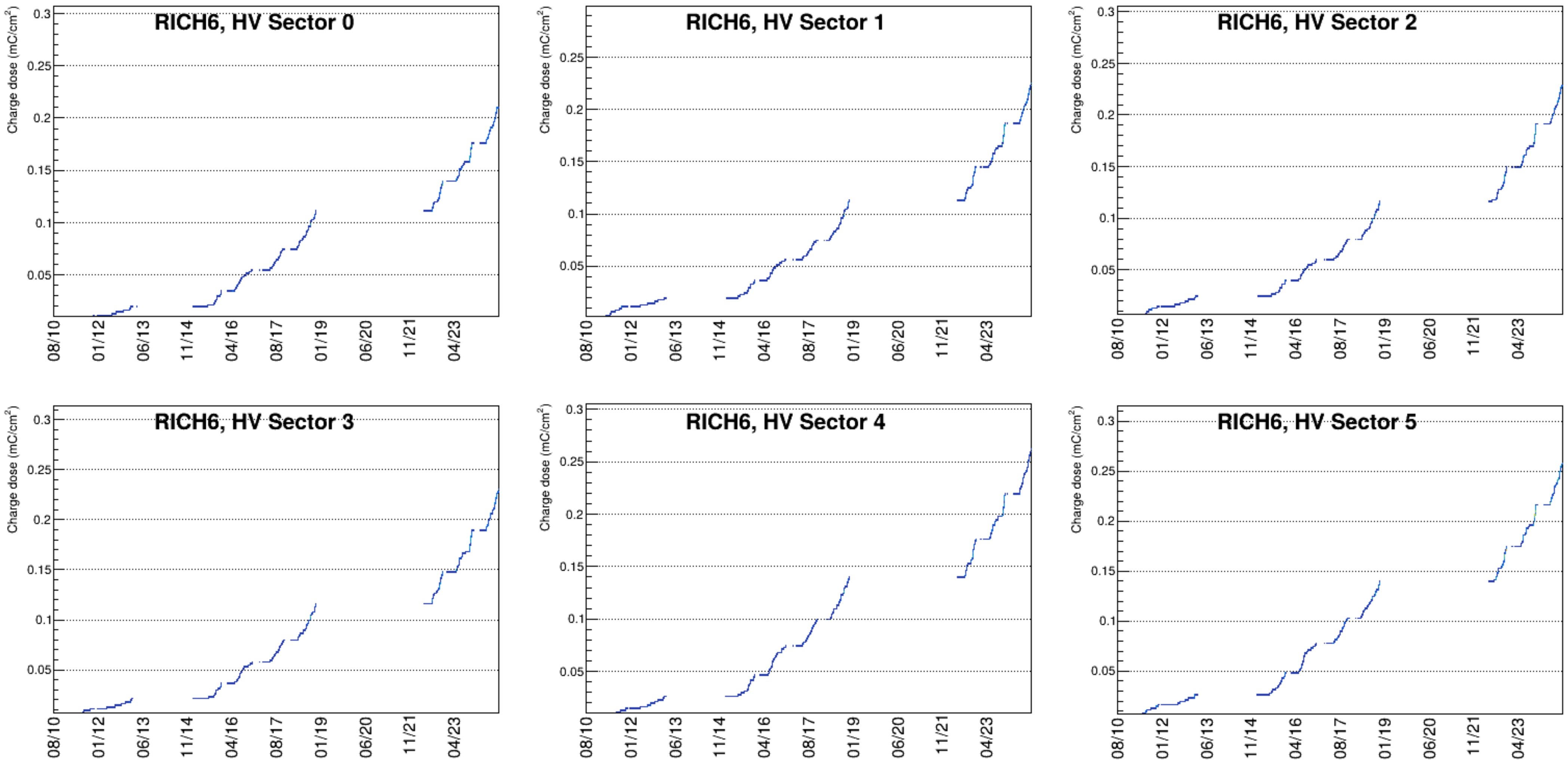

CsI radiation damage: integrated specific charge dose

Absorbed charge dose for HV sector, period 2010 - 2025

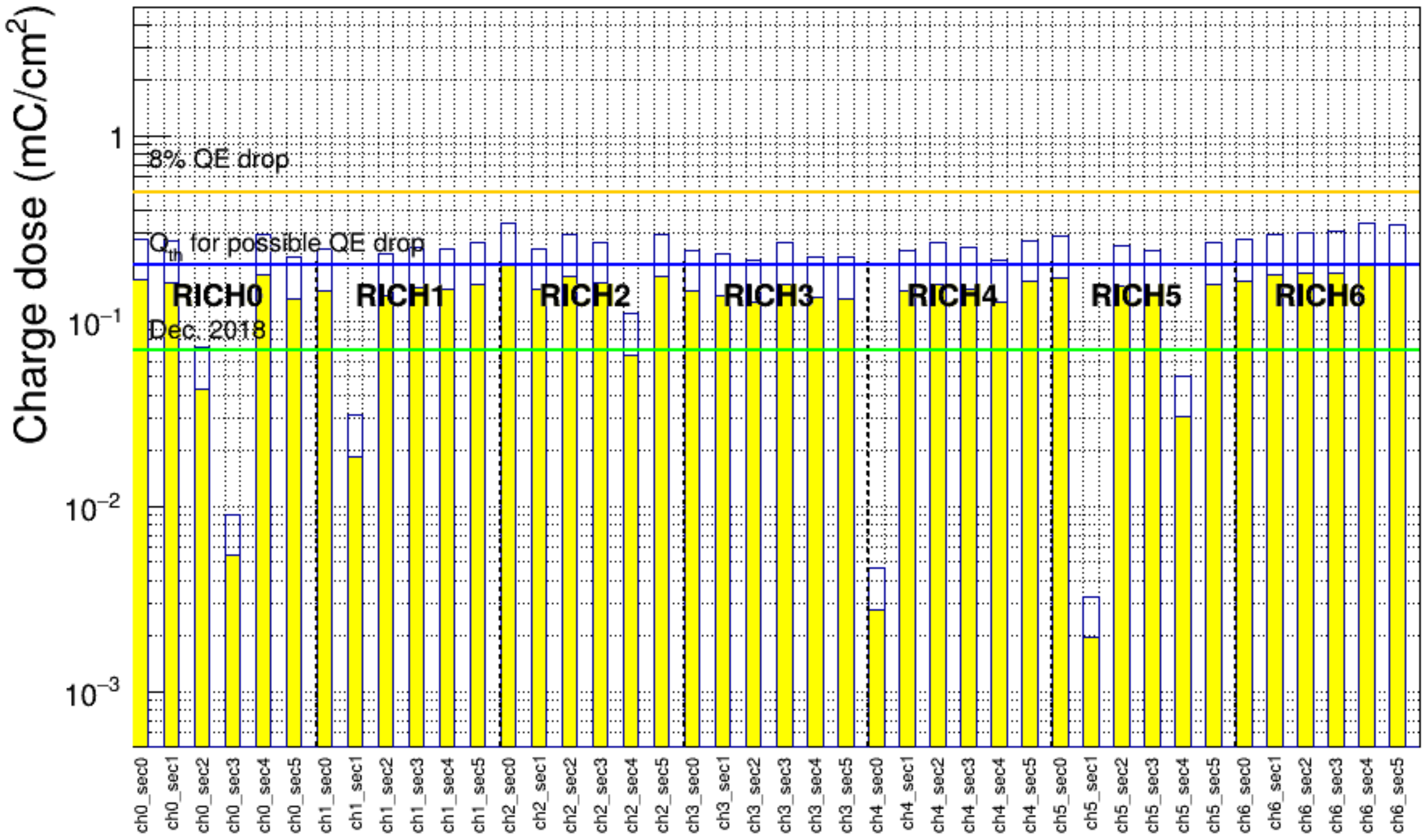

- Full yellow bars: measured CsI charge dose; Empty bars: total anode charge.
- **Bleu line**: dose limit for possible CsI QE loss: 0.2 mC/cm$^{2;}$ [NIM A553 (2015), NIM A574(2007)]
- **Orange line:** 0.44 mC/cm^2 Expected charge dose end RUN 3. Possible CsI QE loss of 8%.

Pattern recognition with the HMPID

- A primary track extrapolated from the internal tracking devices has to match with a MIP cluster. This is mandatory for an efficient reconstruction in events with high occupancy in HMPID
- For every cluster in the event, the Cherenkov angle is evaluated (if exists)
- The photon emission angles are reconstructed using a backtracing loop method
- Background discrimination is performed exploiting the Hough Transform Method (HTM).

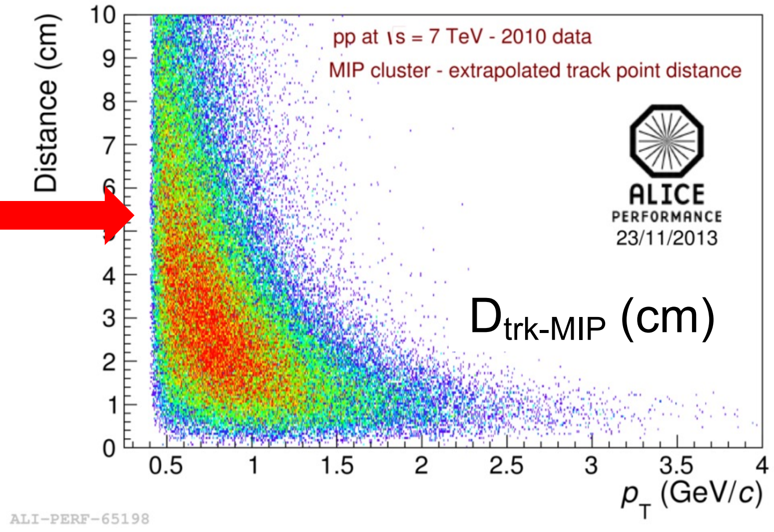

impact track parameter

$$(x,y) \rightarrow ((x_p,y_p,\theta_p,\varphi_p),\ \eta_c)$$

cluster coordinate

Cherenkov angle

$\Downarrow$

solution in one dimensional mapping space η_c

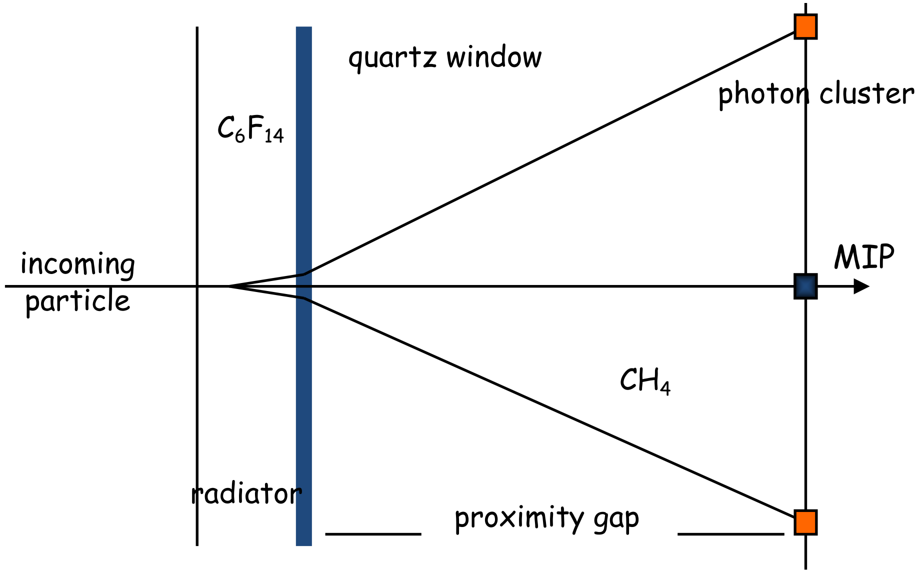

PID performance in Run 1-2

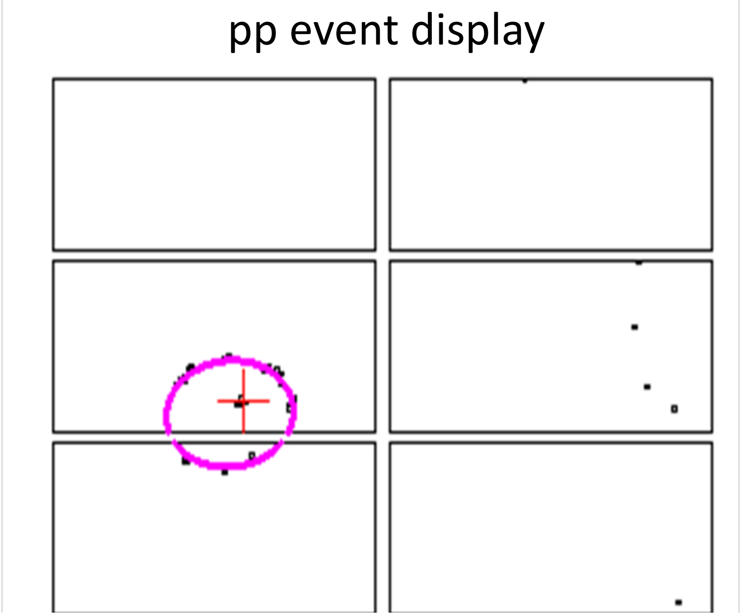

- In pp and p-Pb collisions (low multiplicity events), the results of such a procedure, in a narrow track transverse momentum range, is a three gaussian distribution (π, K and p).

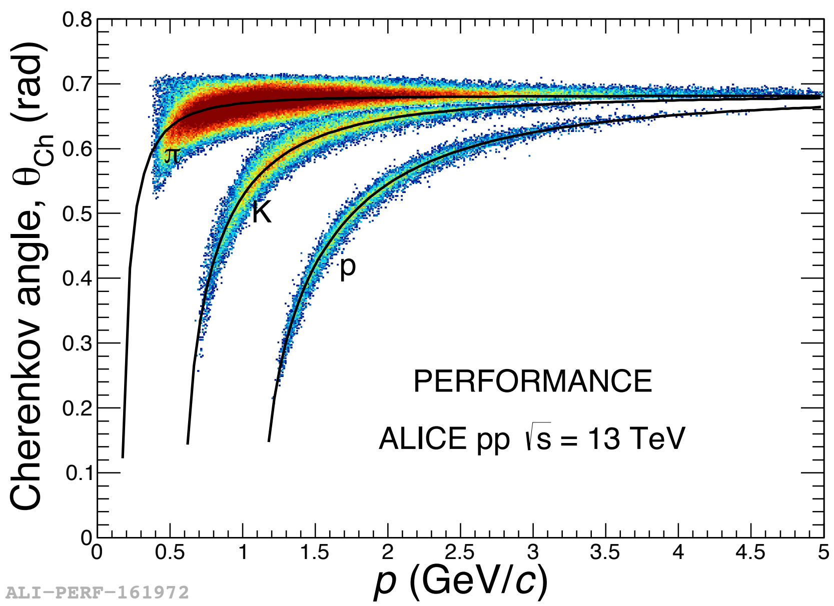

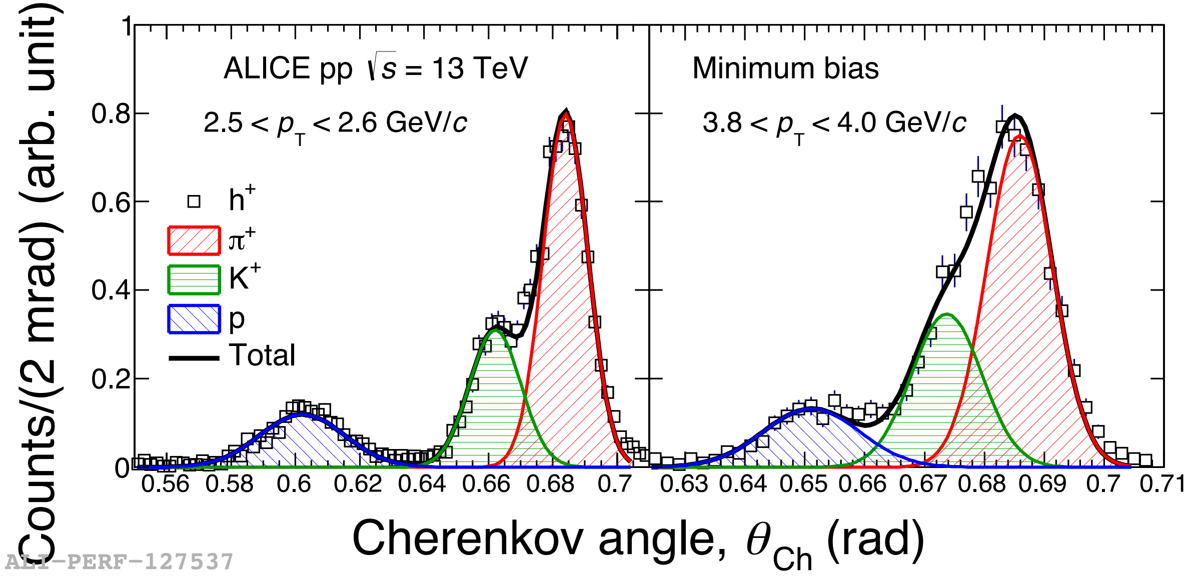

PID performance in Run 1-2

Pb-Pb event display

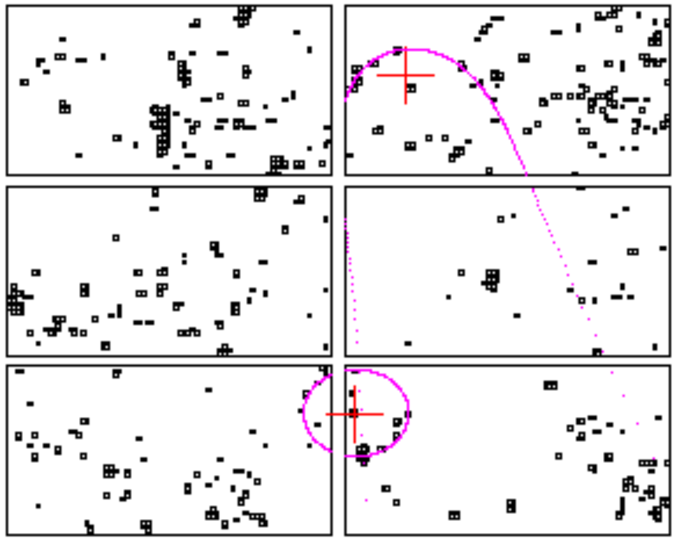

- In pp and p-Pb collisions (low multiplicity events), the results of such a procedure, in a narrow track transverse momentum range, is a three gaussian distribution (π, K and p).

- In the most central Pb-Pb collisions (low multiplicity events), the three Gaussian distributions in a given transverse momentum bins are convoluted with a background distribution;
- Such distribution increases with the Cherenkov angle value;
- It is due to mis-identification in the high occupancy events:
  - larger is the angle value larger is the probability to find background;

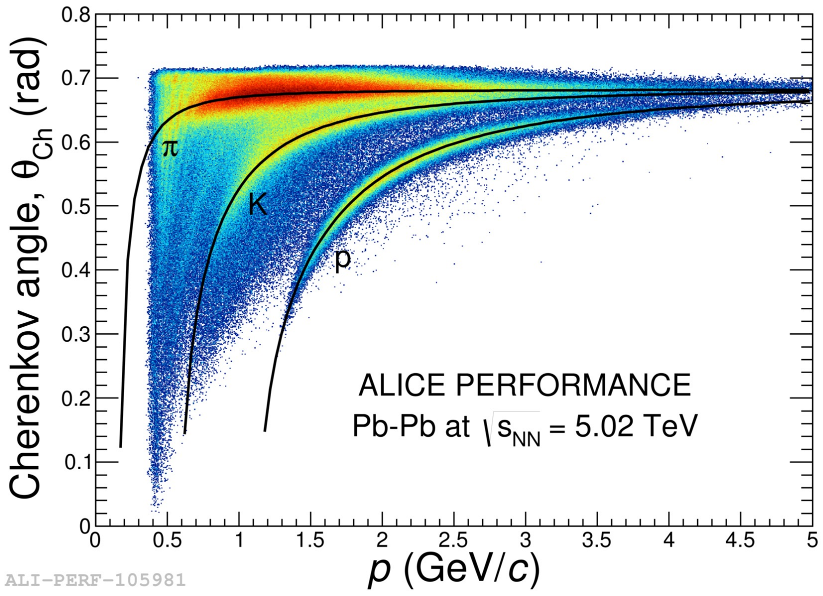

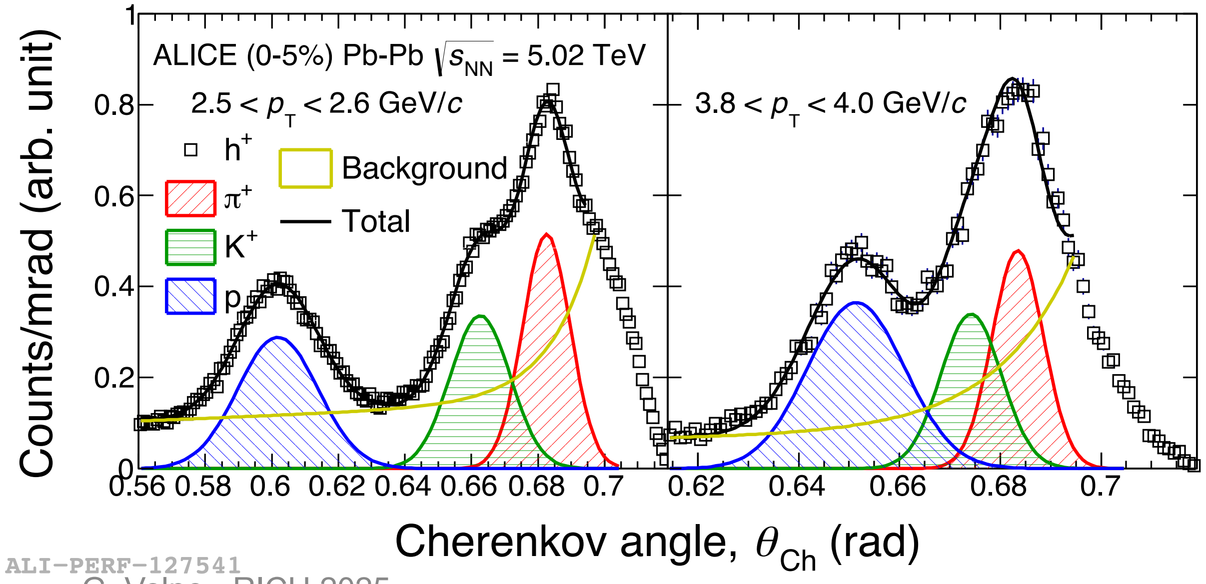

PID performance in Run 3

pp collisions

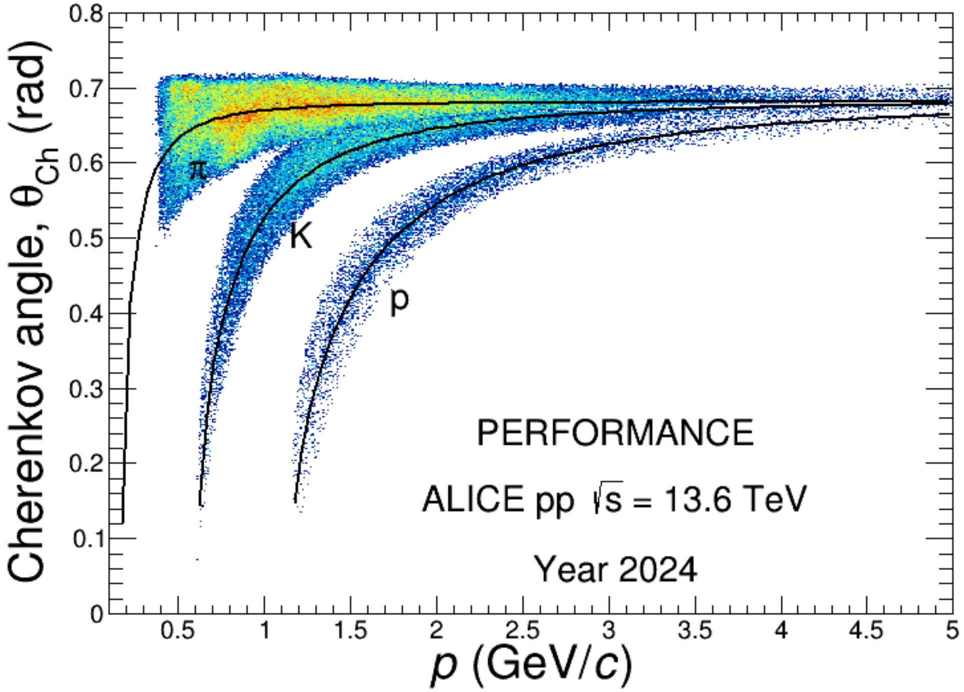

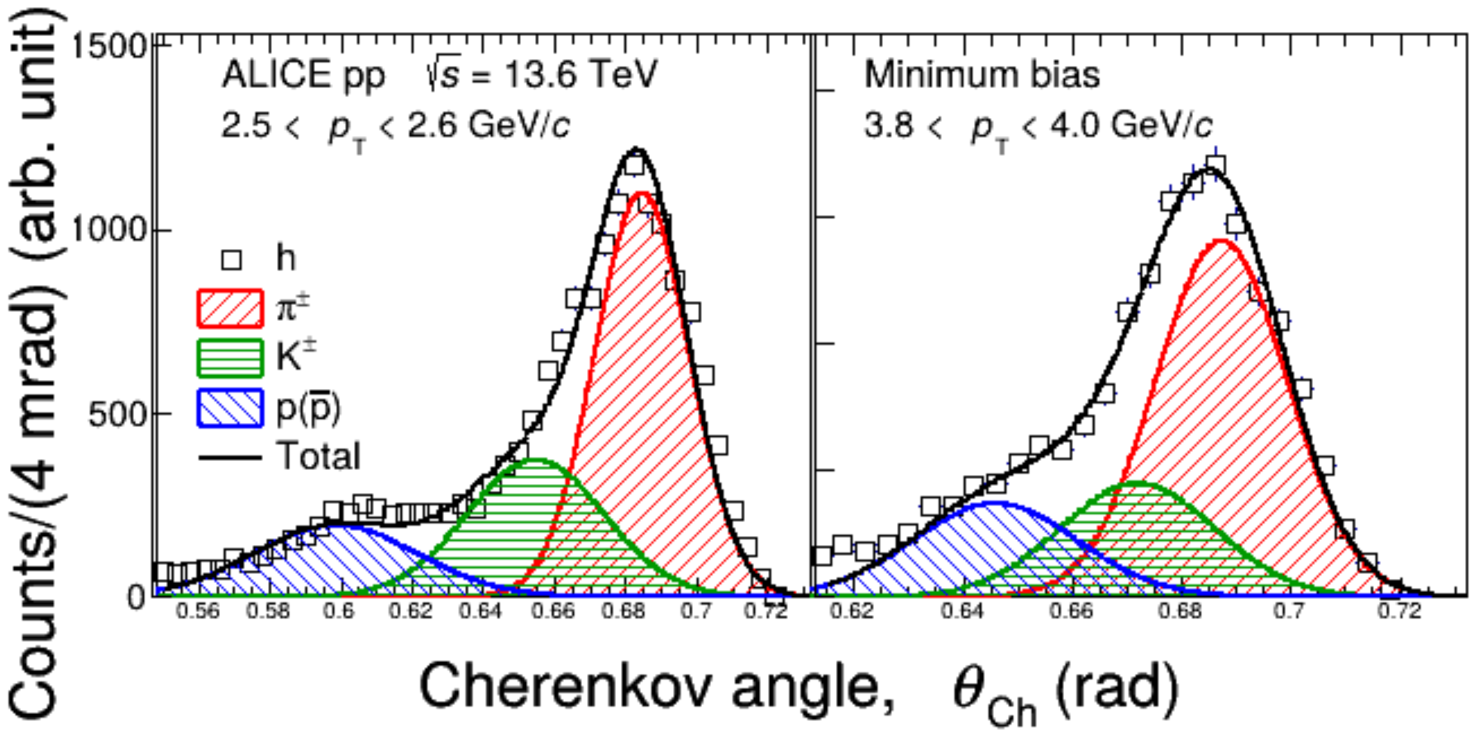

PID performance in Run 3

Pb-Pb collisions (2023)

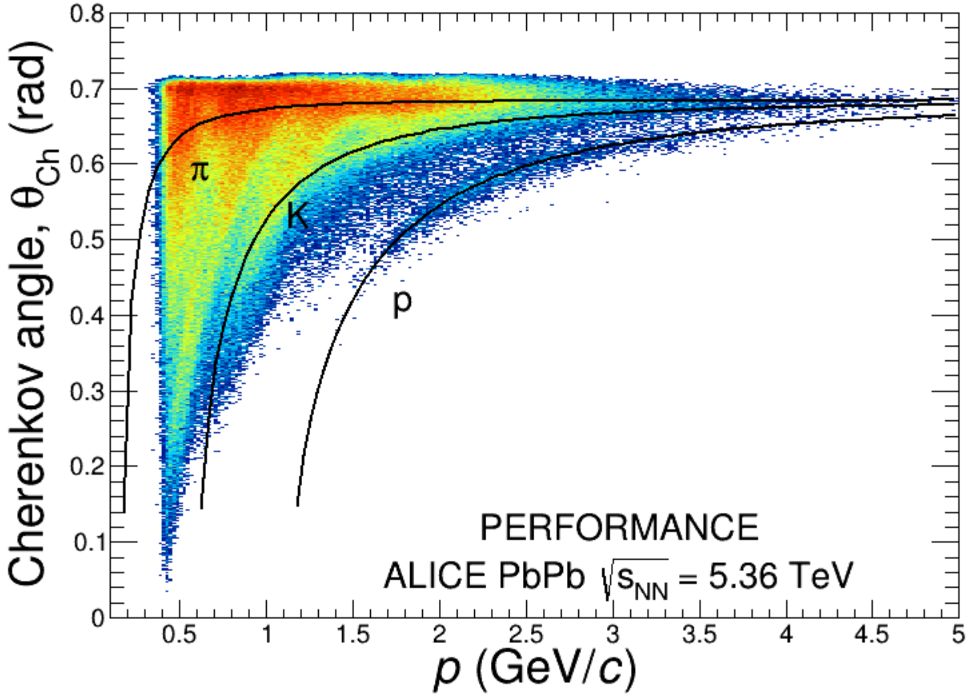

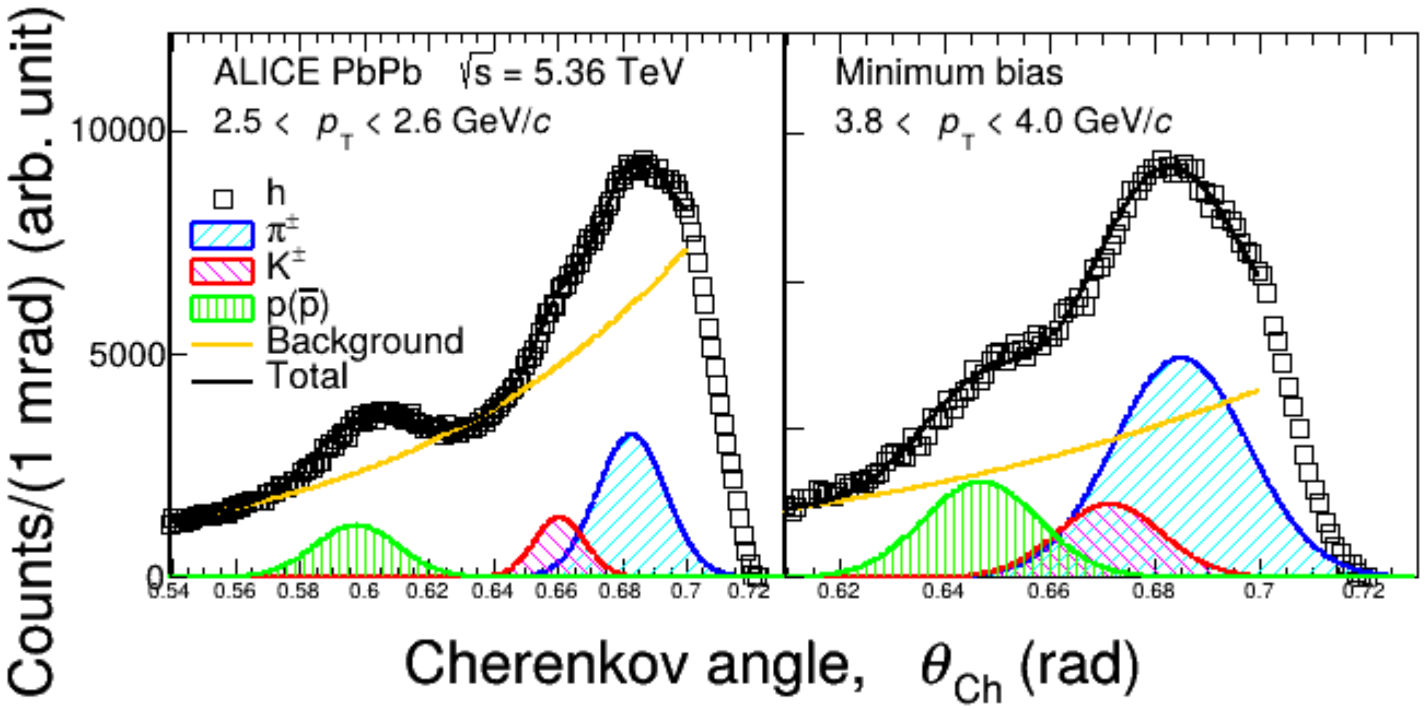

- Higher background w.r.t Run 1-2 data
  - Higher detector occupancy due to the higher events pile-up.
  - Lower number of detected photo-electrons
- Pattern recognition algorithm based on ML approach to improve the PID efficiency are under study.

Absorption cross section measurement

May 2021: installation of the absorbers to measure inelastic cross section of anti-deuterons

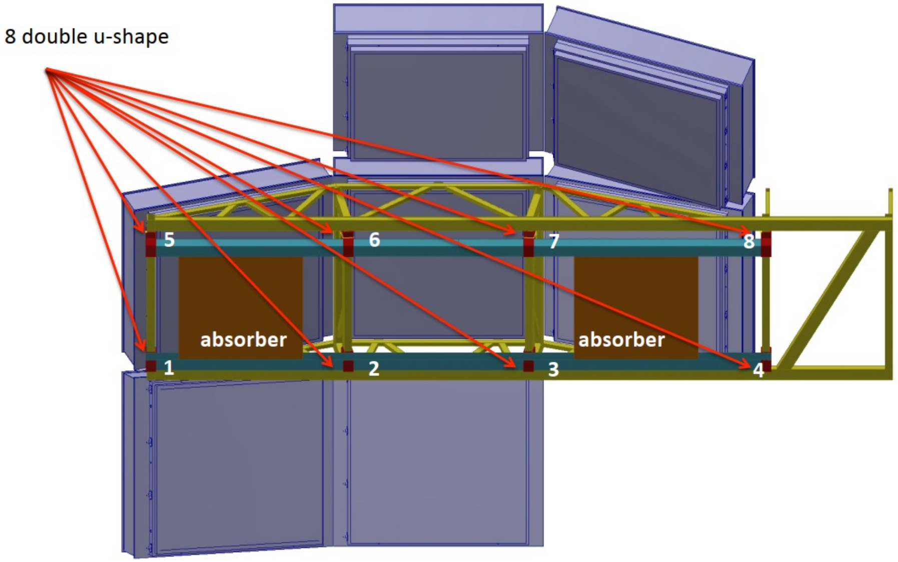

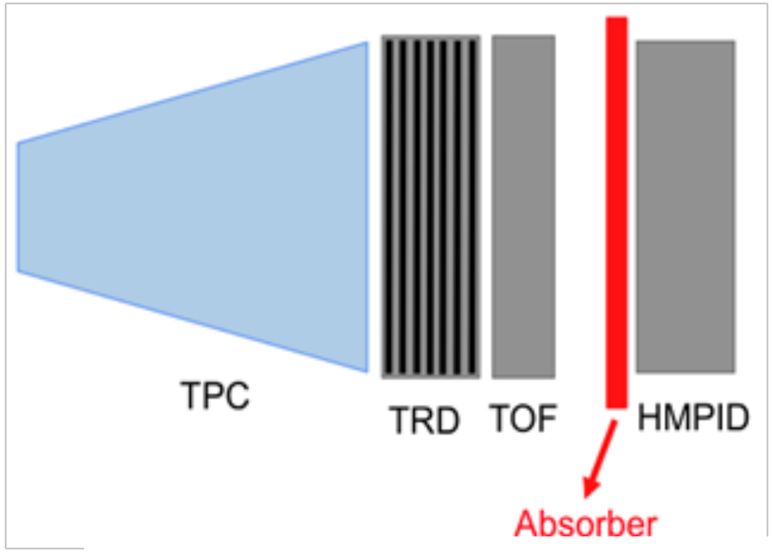

- Interesting for cosmic anti nuclei, multi-baryon state production, constrain to the MC generator...;

- Expected statistical precision 2-4% in the momentum interval 0.2 GeV/*c* < p < 1.4 GeV/*c* for Pb–Pb collisions at √sNN = 5.5 TeV (Run 3)

- A systematic uncertainties of 5.5% is expected based on conservative estimate (https://alice-notes.web.cern.ch/node/1015);

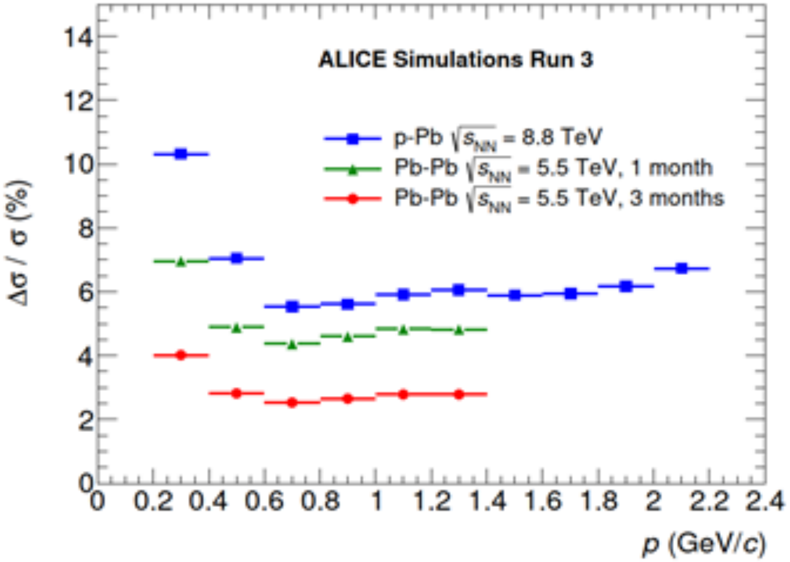

Absorption cross section measurement

- $\mathbf{\Delta r}$ = the distance between the reconstructed MIP track in HMPID and the extrapolated track from the ALICE tracking system.

- The number of surviving (anti-)deuterons will be extracted from the fitting procedure of the $\mathbf{\Delta r}$ distribution using the MC template to discriminate the signal from the background.

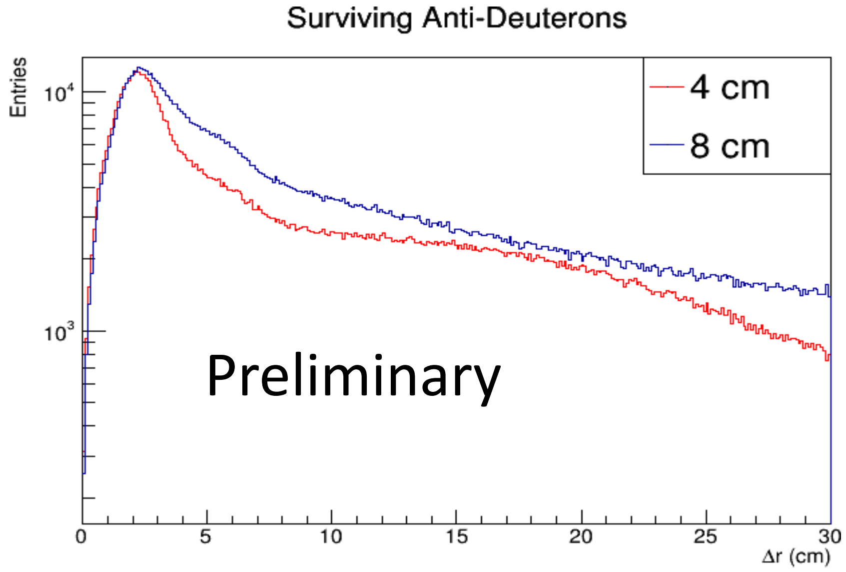

MC template obtained in the case of an 8 cm absorber thickness

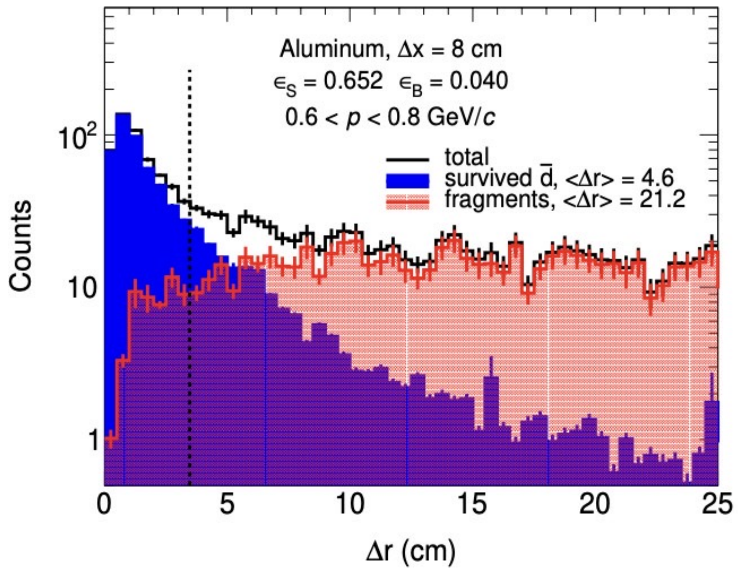

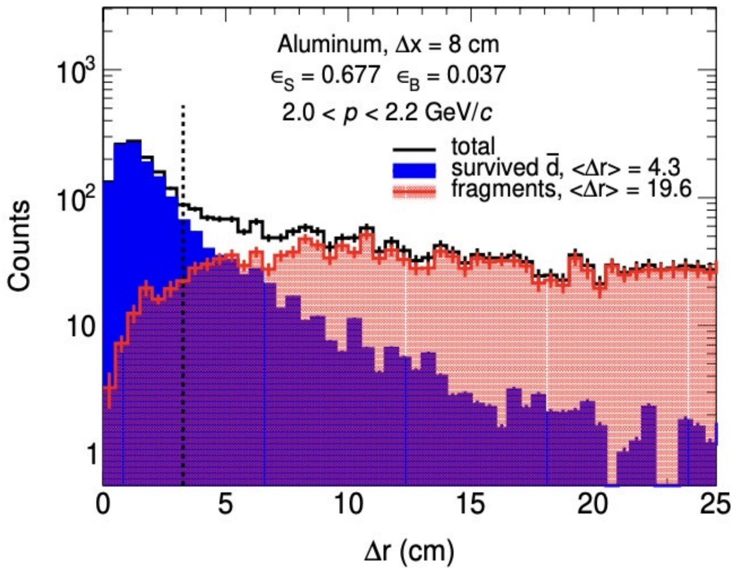

Conclusions

- **The ALICE-HMPID** successfully collected pp and Pb–Pb collision data delivered so far by the LHC during Run 3.
- Currently, the overall detector acceptance has decreased to about 60% due to failures in HV channels and radiator vessels.
- The detector performance, in terms of chamber gain and number of detected photoelectrons, has been evaluated.
  - A decrease in chamber gain has been observed → chambers aging
  - A decrease in average number of detected photo-electrons at saturation has been observed → CsI aging
- The PID performance in Run 3 has also been studied, with no significant degradation detected.
  - However, a higher background level compared to Runs 1 and 2 has been observed, particularly in Pb–Pb collisions, mainly due to higher detector occupancy and lower number of detected photo-electrons.
  - To improve PID efficiency, algorithms based on Machine Learning techniques are currently under study.
- Analysis of charged-particle inclusive production (in particular, light nuclei) has already started.
- The HMPID will be used to measure the absorption cross section of deuterons and antideuterons.

After contributing to LHC Runs 1, 2, and 3, the detector is scheduled to be removed from the ALICE apparatus at the end of Run 3, planned for July 2026.

Backup

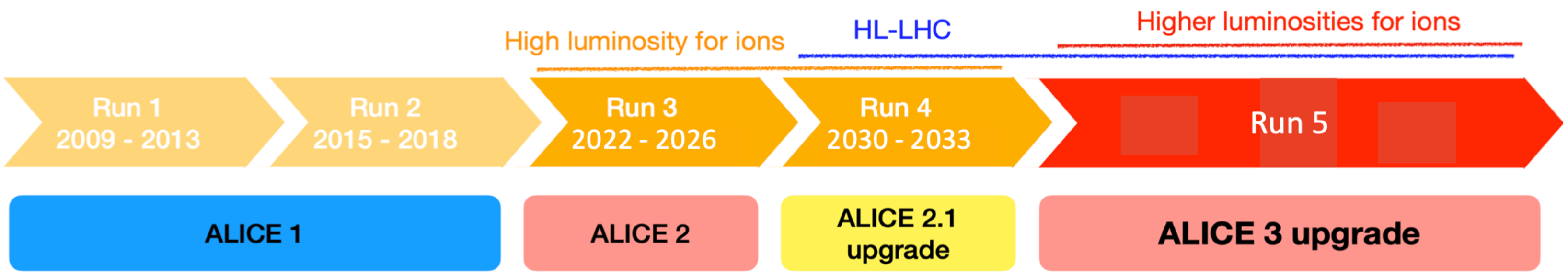
High luminosity for ions
HL-LHC
Higher luminosities for ions
Run 1
2009 - 2013
Run 2
2015 - 2018
Run 3
2022 - 2026
Run 4
2030 - 2033
Run 5
ALICE 1
ALICE 2
ALICE 2.1
upgrade
ALICE 3 upgrade

HMPID detector description

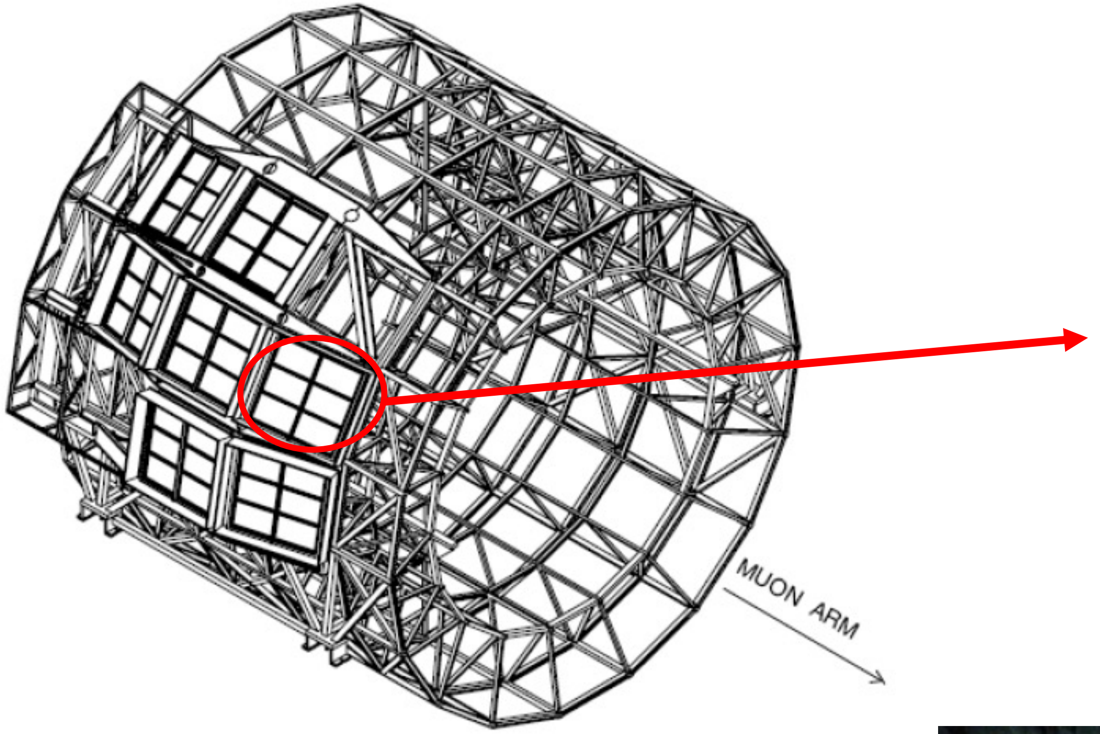

Six photo-cathodes per module

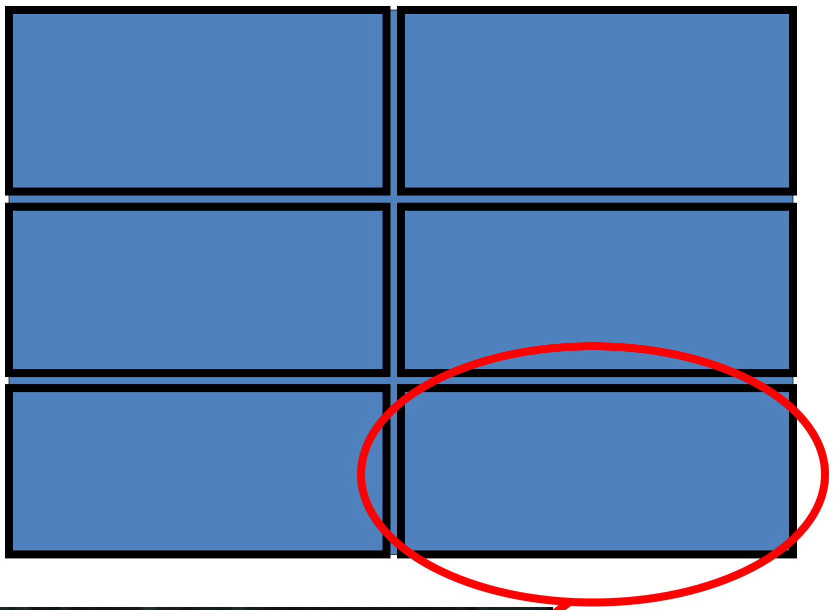

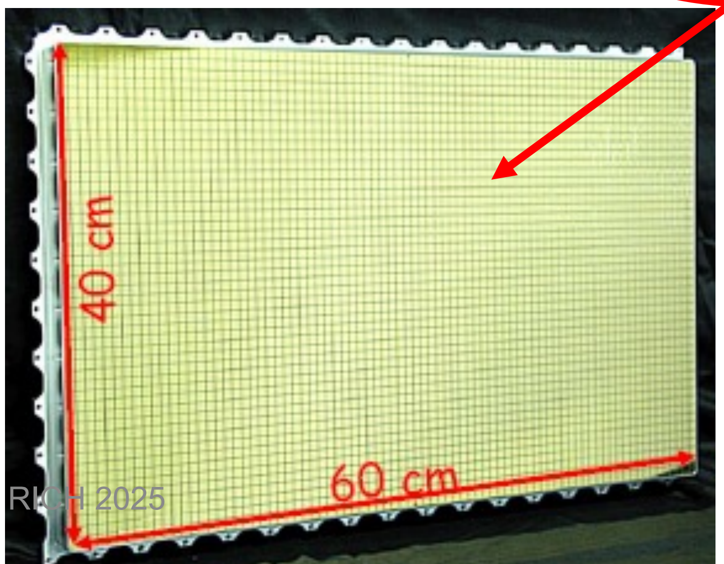

CsI photo-cathode is segmented in 0.8x0.84 cm pads

HMPID detector description

- FEE and RO electronics is based on GASSIPLEX and DILOGIC chips developed within the HMPID project
- GASSIPLEX: 16-channel analogue multiplexed low-noise signal processor, the noise level is 1000 e^-, dead/noisy pads are less than 200 out of 161280
- DILOGIC: individual threshold and pedestal setup
- 42 photo-cathodes are segmented into 3840 pads with individual analog readout.

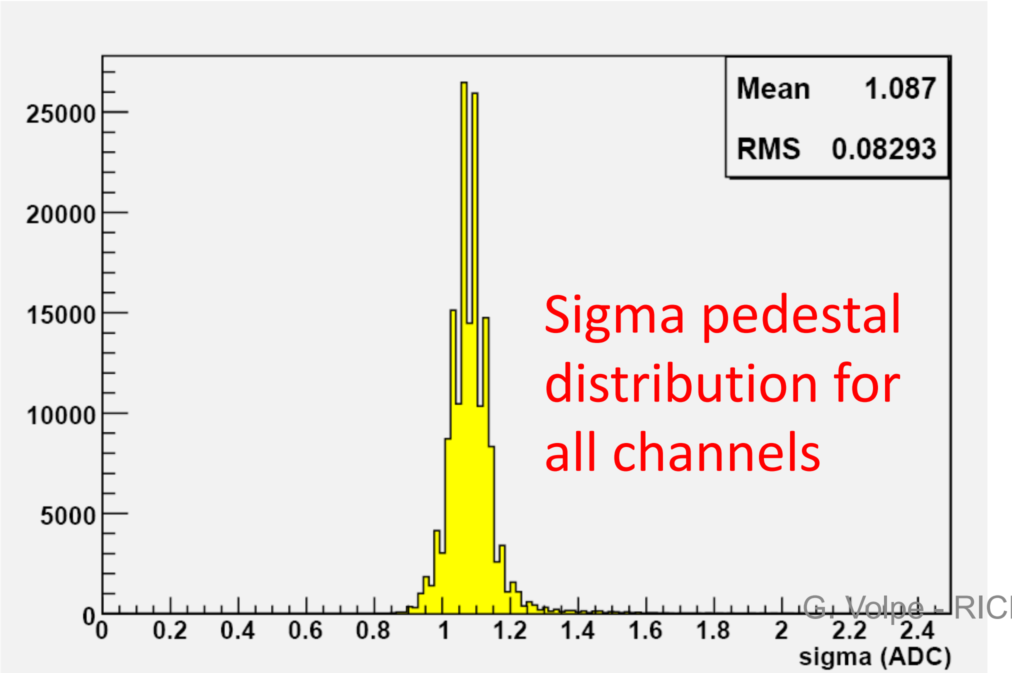

GASSIPLEX DILOGIC

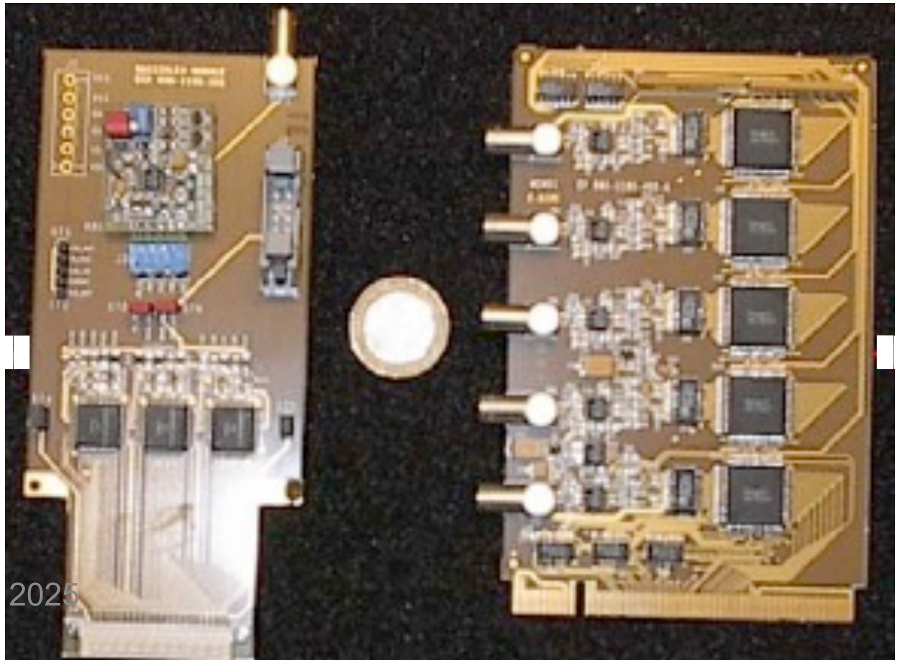

C_6F_{14} circulation, purifying systems and transparency monitoring

- Safe C_6F_{14} circulation by gravity flow;
- Stable transparency to Cherenkov photons;
- Separated control for each radiator vessel;

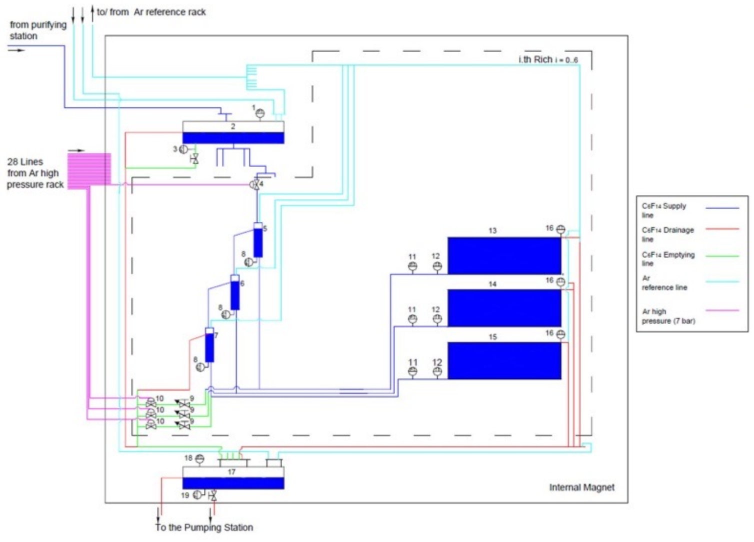

Fig 10 Schematic of the distribution station for one module.

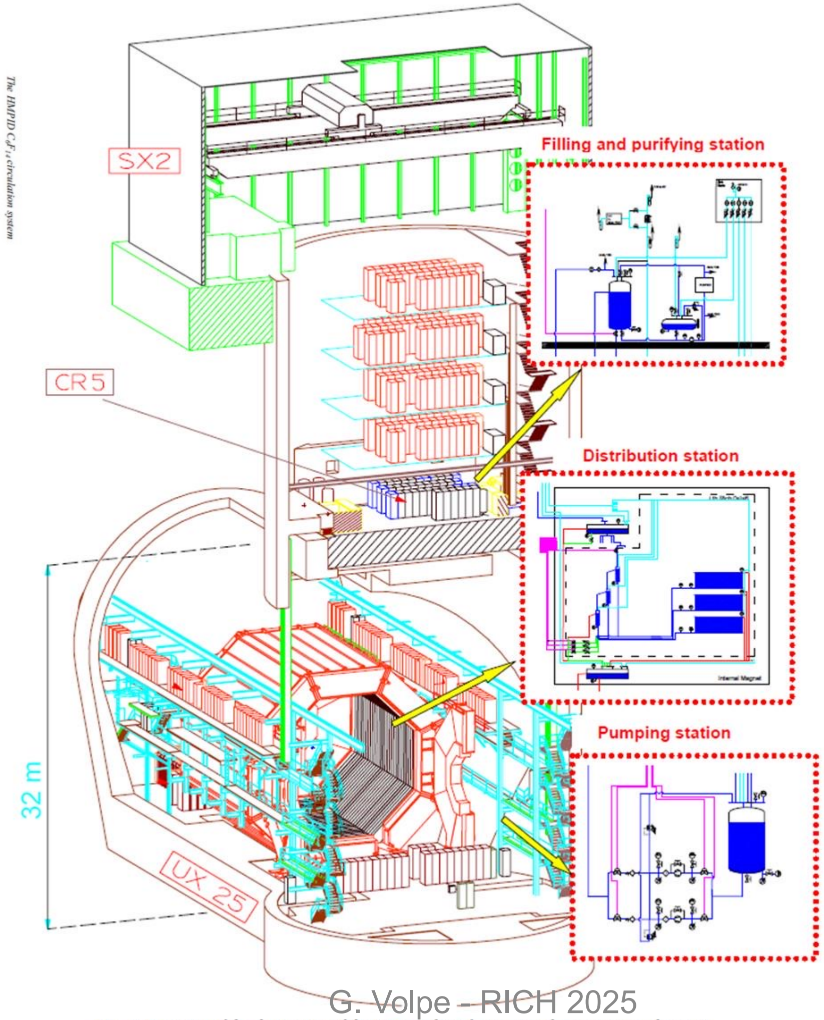

Fig. 6 Location of the three units of the HMPID liquid system in the experimental cavern.

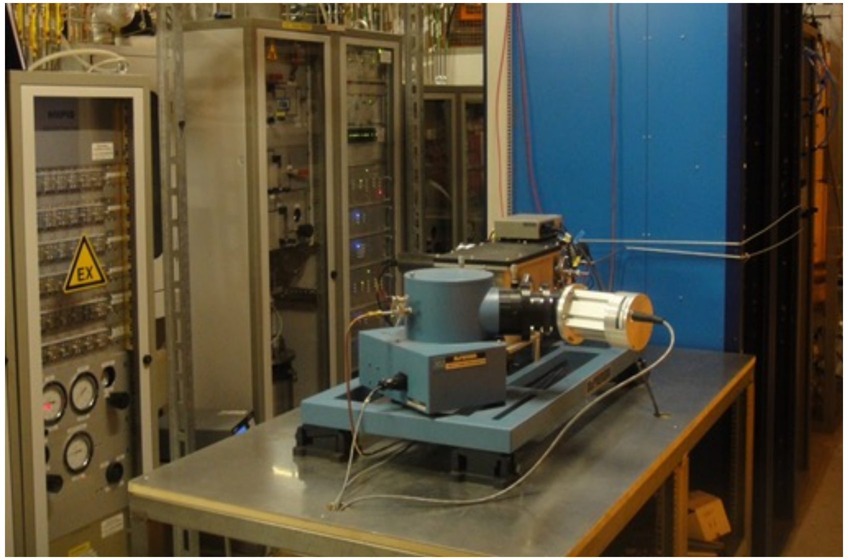

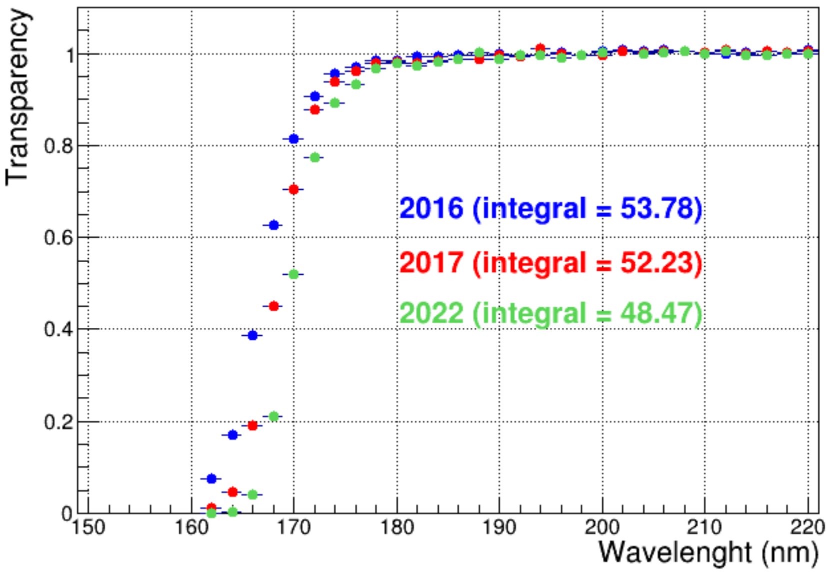

Pattern recognition with the HMPID

Background discrimination is performed exploiting the Hough Transform Method (HTM).

• HTM is an efficient implementation of a generalized *template matching* strategy for detecting complex patterns in binary images.

• The starting point of the analysis is a bi-dimensional map with the impact point (x_p, y_p) of the charged particles, hitting the detector plane with known incidence angles (θ_p, φ_p), and the coordinates (x, y) of hits due to both Cherenkov photons and background sources.

• A "Hough counting space" is constructed for each charged particle, according to the following transform: $(x, y) \rightarrow ((x_p, y_p, \theta_p, \varphi_p), \eta_c)$

• (x_p, y_p, θ_p, φ_p) is provided by the tracking of the charged particle, so the transform will reduce the problem to a solution in a one-dimensional mapping space.

• A η_c bin with a certain width is defined. The Cherenkov angle θ_c of the particle is provided by the average of the η_c values that fall in the bin with the largest number of entries

PID performance

Identification on statistical basis: low multiplicity events

the particle yields are evaluated from a three-Gaussian fit to the Cherenkov angle distribution in a narrow transverse momentum range. The function used is the following:

$$f(\theta) = \frac{Y_\pi}{\sigma_\pi \sqrt{2\pi}} e^{-\frac{(\theta - \langle\theta_\pi\rangle)^2}{2\sigma_\pi^2}} + \frac{Y_K}{\sigma_K \sqrt{2\pi}} e^{-\frac{(\theta - \langle\theta_K\rangle)^2}{2\sigma_K^2}} + \frac{Y_p}{\sigma_p \sqrt{2\pi}} e^{-\frac{(\theta - \langle\theta_p\rangle)^2}{2\sigma_p^2}}$$

$<\theta_i>$ = means of the Cherenkov angle distributions
σ_i, = standard deviation of the Cherenkov angle distributions.
Y_i = integral of the single Gaussian functions

- 9 parameters to be calculated, the three mean values, the three sigma values and the three yields.
- Mean and sigma values are known and fixed in the fitting.

pp event display

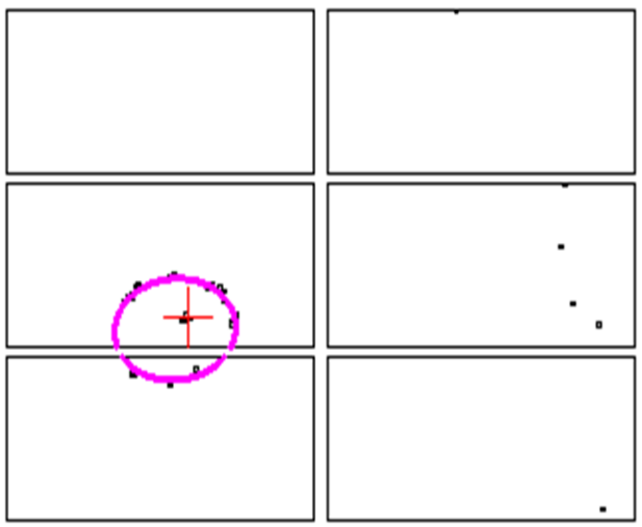

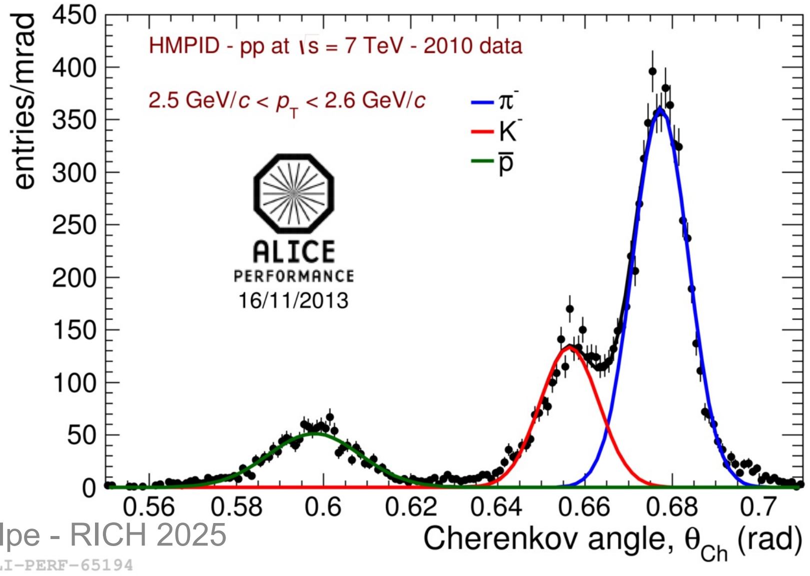

PID performance

Identification on statistical basis: high multiplicity events (central Pb-Pb collisions)

- the three Gaussian distributions in a given transverse momentum bins are convoluted with a background distribution;
- Such distribution increases with the Cherenkov angle value;
- It is due to mis-identification in the high occupancy events:
    - larger is the angle value larger is the probability to find background;
- In the yield extraction procedure, the background function has to be convoluted with the three-Gaussian one.

Pb-Pb event display